Obtaining amplitude-modulated bursting by multiple-frequency slow parametric modulation

Xiujing Han,[1,*] Mengke Wei,[1] Qinsheng Bi,[1] and Jürgen Kurths[2,3]
[1]*Faculty of Civil Engineering and Mechanics, Jiangsu University, Zhenjiang Jiangsu 212013, People's Republic of China*
[2]*Department of Physics, Humboldt University, Berlin 12489, Germany*
[3]*Potsdam Institute for Climate Impact Research, Potsdam 14473, Germany*

(Received 29 October 2017; published 3 January 2018)

Amplitude-modulated bursting (AMB), characterized by oscillations appearing in the envelope of the active phase of bursting, is a novel class of bursting rhythms reported recently. The present paper aims to report a simple and effective method, i.e., the multiple-frequency slow parametric modulation (MFSPM) method, for obtaining such a bursting pattern. We show that the MFSPM can be well controlled so that it may exhibit multiple continuous ups and downs in the active area. Then, the amplitude of the traced active state alternates between increases and decreases accordingly, which leads to oscillations in the envelope of the active phase, and AMB is thus created. Based on this, the route to AMB by the MFSPM is presented. The validity of the approach is demonstrated by several examples. The proposed approach does not depend on specific systems or bifurcations and thus is a general method.

DOI: 10.1103/PhysRevE.97.012202

I. INTRODUCTION

The slowly varying control parameter problem may be encountered in many practical applications, for example, the catalytic activities in chemical reactors [1], the spike oscillations in reaction-diffusion systems [2], and the stabilization and control of dynamical systems [3,4], where the slow parameter is experimentally controlled or actually a slowly varying variable. As one of the most common hypotheses describing the variety law of the slow parameter, slow harmonic modulation of the control parameter has been found to have great effects on dynamical behaviors of a system. For example, slow harmonic modulation may help us to track unstable periodic orbits [5], control coexisting attractors [6], and annihilate one of the coexisting states [7]. It has also been shown that slow harmonic modulation is a useful tool to stabilize unstable orbits [8] and lead the system from chaos to order [9]. In particular, the related topic involving dynamic bifurcations has received much attention. Bifurcation delay behaviors, i.e., the delay loss of stability of attractors, resulted from the slow passage through bifurcation points of the system [10–12], are interesting dynamical phenomena related to this. Based on bifurcation delay, many types of bursting have been revealed [13–15].

Bursting is a complex, multiple-time-scale dynamical behavior and is ubiquitous in almost every field of science [16–19]. Amplitude-modulated bursting (AMB) refers to a class of interesting bursting rhythms. Such bursting pattern, characterized by the novel dynamical characteristics, that is, distinct oscillations appear in the envelope of the active phase, was first reported by Vo *et al.* [20] when they studied a model for the intracellular calcium dynamics recently. It has been shown that the AMB results from torus canard dynamics, a novel class of singularities for differential equations. Because torus canards can be observed in many dynamical models [21–24], it is believed that it may be possible to observe AMB in many other dynamical systems or even in experiments.

Here, we consider ordinary differential equations, written in the general form

$$\dot{x} = F(x,\lambda), \tag{1}$$

where $x \in \mathbb{R}^n$ is the vector of dynamics and $\lambda \in \mathbb{R}$ is one of the parameters of the system. We assume that system (1) has only one time scale; i.e., fast-slow characteristics cannot be observed in the system. Then, λ is chosen to be the time-dependent parameter to which the slow modulation is applied in the form

$$\lambda = \alpha + \beta_1 \cos(\omega_1 t) + \beta_2 \cos(\omega_2 t), \tag{2}$$

where $\alpha \in \mathbb{R}$ is the control parameter and $\beta_1\cos(\omega_1 t)$ and $\beta_2\cos(\omega_2 t)$ are slow parametric excitations with the modulation frequencies $\omega_{1,2} \ll 1$. The slow modulation (2) studied here shows multiple frequency components and thus can be referred to as a multiple-frequency slow parametric modulation (MFSPM), which is quite different compared to the slow modulations studied in previous works (e.g., see [1–12]). Because the frequencies $\omega_{1,2}$ are small, the presence of the MFSPM may lead to fast-slow characteristics, and as a result, bursting may be created in the system.

The present work focuses on the generation of AMB by using the MFSPM. We explain how AMB is generated in a simple and controllable way. In particular, we show that AMB may be ubiquitous in dynamical systems modulated by the MFSPM; therefore, torus canards are not necessary conditions for the generation of AMB. The rest of this paper is organized as follows. In Sec. II, we present the basic idea for obtaining AMB. Then, in Sec. III, several examples of AMB induced by the MFSPM are explored. Finally, in Sec. IV, we conclude with a discussion of the results.

*xjhan@mail.ujs.edu.cn

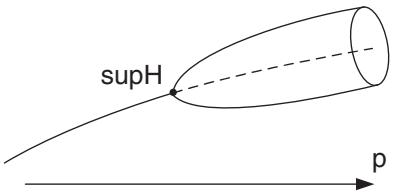

FIG. 1. In this schematic diagram, the stable limit cycle, resulting from a supercritical Hopf bifurcation (supH), grows gradually as the control parameter increases.

II. BASIC APPROACH

Bursting, as we know, can be observed when the activity of a system undergoes transitions between a rest state and an active state. Here the active state is often associated with a limit cycle attractor [16,25], an extremely common kind of attractor in dynamical systems. When the bursting trajectory switches from the rest state to the active state, the active phase of bursting (i.e., the large-amplitude oscillations in bursting) takes place, and it will not disappear until the trajectory jumps back to the rest state. On the other hand, as mentioned earlier, the active phase of AMB shows interesting features; i.e., distinct oscillations appear in the envelope. Therefore, in order to obtain AMB, the amplitude of the traced active state should vary constantly during the active phase of bursting.

The traced active state, as a periodic attractor, shows amplitude which often varies with system parameters. However, the related variety laws are usually simple, e.g., the amplitude increases with the parameters (see Fig. 1), which thus cannot directly lead to fluctuations in the envelope of the active phase.

In fact, a fluctuation can be induced in the envelope by a slow parametric modulation even based on a simple variety law of the amplitude of the active state. In order to provide a clear illustration of this idea, we consider an instructive example involving a modified circuit system [26,27],

$$\dot{x} = -c(x^3 - dx - y), \quad \dot{y} = x - ay - z, \quad \dot{z} = by, \qquad (3)$$

where a, b, and c are the parameters and $d = \beta\cos(\omega t)$ is the single-frequency slow parametric modulation. According to [14], a bursting pattern, classified as "subHopf/fold cycle" bursting, is observed in the system [e.g., see Figs. 2(a) and 2(b)]. Here we focus on the active phase of this bursting pattern. As shown in Fig. 2(c), when the trajectory switches to the active state by the subcritical Hopf bifurcation subH, the active phase is triggered. Then, a decreasing of the slow parameter $\beta\cos(\omega t)$ [i.e., the function $0.84\cos(0.01t)$] leads the amplitude of the active state to decrease, and this accounts for the evolution process that the envelope gets narrow gradually [see Fig. 2(b)]. After reaching its minimum, $\beta\cos(\omega t)$ begins to increase. As a result, the amplitude of the active state increases accordingly, and this gives rise to the second evolution process that the envelope becomes wider gradually [see Fig. 2(b)]. These two evolution processes form a fluctuation, and in particular, the connection point of the two evolution processes indicates an extreme point in the envelope of the active phase.

The existence of extreme points is the evidence for oscillations. Therefore, in order to obtain AMB, more than one extreme point should be created in the envelope of the active phase. This may be realized by finding a proper slow parameter,

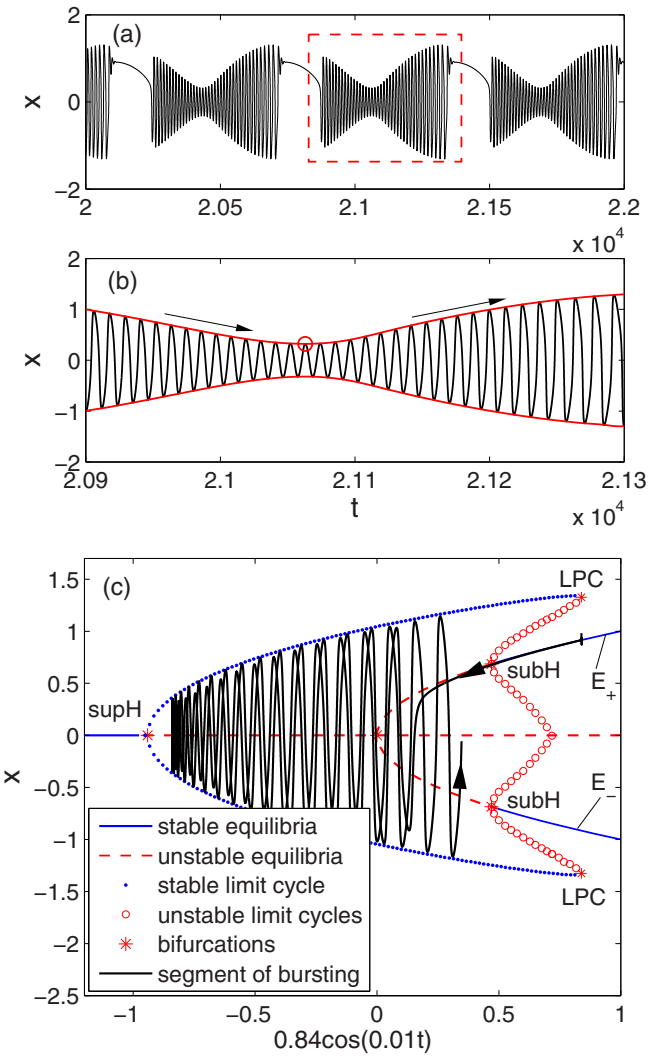

FIG. 2. "SubHopf/fold cycle" bursting (a),(b) and its fast-slow analysis (c) in system (3), where the parameters are the same as in Fig. 10 of Ref. [14]. An enlargement of (a) is shown in (b), where the circle means an extreme point of the envelope (red curve). supH, supercritical Hopf bifurcation; subH, subcritical Hopf bifurcation; LPC, fold bifurcation of limit cycles; $E_{\pm}$, nonzero equilibrium points.

which alternates between increase and decrease during the active phase of bursting. The MFSPM given by (2) is exactly such a slow parameter if the following two conditions are satisfied (e.g., see Fig. 3).

(a) The control parameter α and the excitation amplitude β_1 are selected properly so that the slow parameter $\alpha + \beta_1\cos(\omega_1 t)$ is able to visit the designated rest and active areas.

(b) The excitation $\beta_2\cos(\omega_2 t)$ is selected properly so that the MFSPM fluctuates narrowly around $\alpha + \beta_1\cos(\omega_1 t)$ in the rest and active areas. Specifically, ω_2 is an integer multiple of ω_1; i.e., $\omega_2 = n\omega_1$, where $n > 1$ is a positive integer. β_2 is relatively small so that the MFSPM can only visit the rest and active areas.

Condition (a) means that the system will undergo transitions between the rest and active states, and thus a common bursting pattern may be created. When the excitation $\beta_2\cos(\omega_2 t)$ whose frequency is an integer multiple as that of $\beta_1\cos(\omega_1 t)$ is added

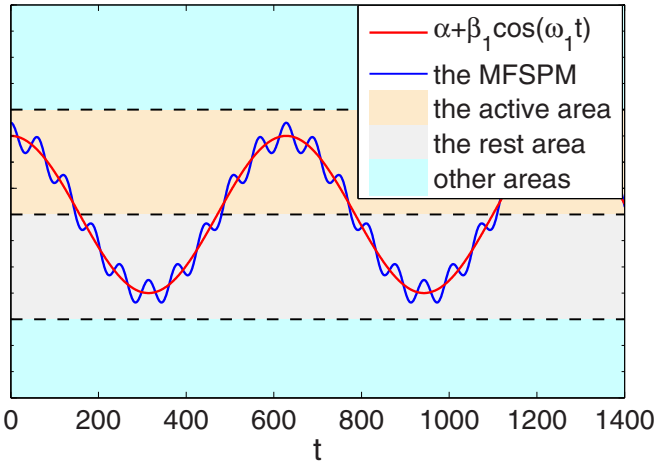

FIG. 3. In this schematic diagram, the MFSPM and its overlay with $\alpha + \beta_1\cos(\omega_1 t)$. The slow parameter $\alpha + \beta_1\cos(\omega_1 t)$ can be easily controlled so that it is able to visit the designated rest and active areas. Then the additional slow excitation $\beta_2\cos(\omega_2 t)$ with a relatively high frequency ($\omega_2 = n\omega_1$, where $n > 1$ is an integer) and smaller amplitude may lead to multiple continuous ups and downs in the active area. Based on this, AMB will appear.

to $\alpha + \beta_1\cos(\omega_1 t)$, surely the resultant MFSPM will exhibit multiple ups and downs during each period. However, the rest and active areas are likely to be small and limited (see Fig. 3). Therefore, in order to make sure that the MFSPM can visit nothing except the designated rest and active areas, the amplitude β_2 should be relatively small. If so, multiple continuous ups and downs can be observed in the active area, which thus leads to multiple extreme points in the envelope of the active phase, i.e., the envelope of the active phase shows oscillations. As a result, AMB is created.

III. EXAMPLES

Bursting results from the transitions between the rest and active states, and the transitions are often modulated by bifurcations, in which Hopf bifurcation is the most studied bifurcation behavior in relation to bursting. In this section, based on Hopf bifurcation, several examples of AMB will be explored by using the MFSPM method.

Example 1. We consider the normal form of a supercritical Hopf bifurcation, given by [28]

$$\dot{x} = ax - y - x(x^2 + y^2),$$
$$\dot{y} = x + ay - y(x^2 + y^2), \tag{4}$$

where a is the control parameter. The supercritical Hopf bifurcation takes place at $a = 0$, which divides the parameter axis a into two parts. $a > 0$ means the active area where there is a stable limit cycle, while $a < 0$ indicates the rest area where there is a stable equilibrium point.

In order to obtain AMB, we substitute the MFSPM for the parameter a; i.e., $a = \alpha + \beta_1\cos(\omega_1 t) + \beta_2\cos(\omega_2 t)$, where the parameters α, $\beta_{1,2}$, and $\omega_{1,2}$ can be determined according to conditions (a) and (b). Then Fig. 4 shows a group of bursting patterns with increasing values of ω_2 for fixed $\alpha = 1$, $\beta_1 = 3$, $\omega_1 = 0.01$, and $\beta_2 = 1$. Obviously, $a = \alpha + \beta_1\cos(\omega_1 t) + \beta_2\cos(\omega_2 t)$ becomes a single-frequency slow parametric modulation if $\omega_2 = \omega_1 = 0.01$. For this case, the slow parameter a is not able to show multiple ups and downs in the active area during each period [see Fig. 5(a)], and therefore AMB cannot be obtained; instead, a common bursting pattern is created [see Fig. 4(a)].

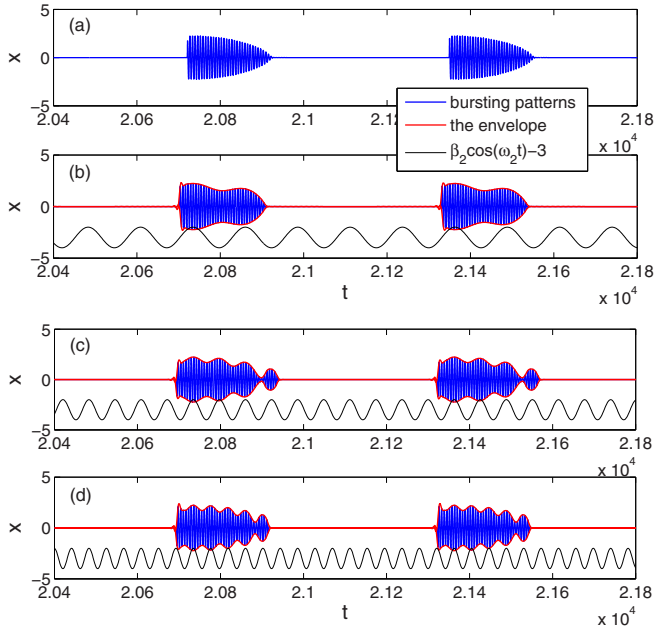

FIG. 4. Transition from (a) a common bursting pattern to (b)–(d) the AMB patterns. (a) $\omega_2 = 0.01$, (b) $\omega_2 = 0.05$, (c) $\omega_2 = 0.1$, and (d) $\omega_2 = 0.15$. In (b)–(d), the function $\beta_2\cos(\omega_2 t) - 3$ is superimposed, which gives a clear view that $\omega_e = \omega_2$.

When the frequency ω_2 is increased, the case, however, is quite different. That is, during each period, multiple continuous ups and downs are observed in the active area [e.g., see Figs. 5(b)–5(d)], which leads to oscillations in the envelope

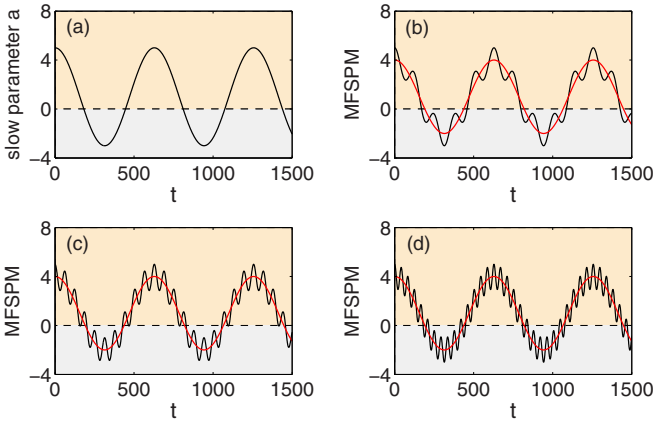

FIG. 5. Evolutions of (a) the single-frequency slow parameter and (b)–(d) the MFSPM. The parameters in (a), (b), (c), and (d) are the same as in Figs. 4(a), 4(b) 4(c), and 4(d), respectively. Yellow region, the active area; gray region, the rest area. In (b)–(d), the function $\alpha + \beta_1\cos(\omega_1 t)$ (red curve) is superimposed, clearly showing the narrow fluctuations that the MFSPM exhibits.

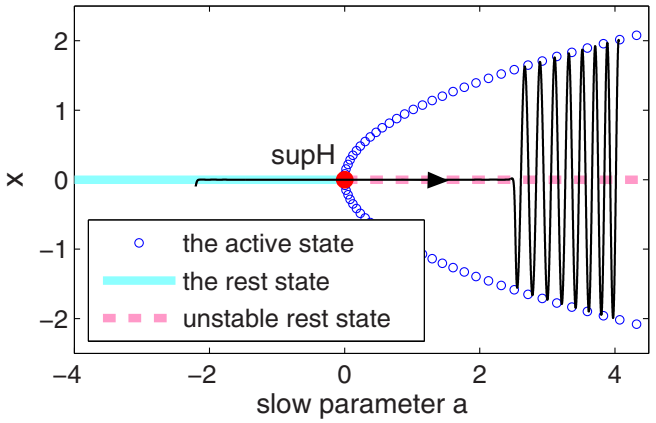

FIG. 6. Numerical simulation of the Hopf bifurcation delay in system (4), where the slow parameter a is the same as in Fig. 4(a).

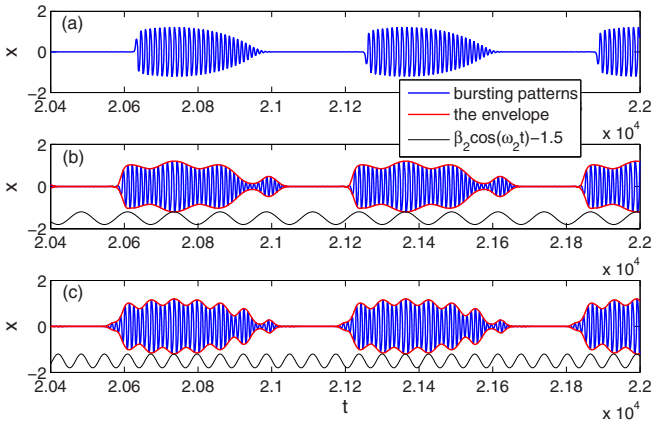

FIG. 7. The same as in Fig. 4 for system (3). (a) $\omega_2 = 0.01$, (b) $\omega_2 = 0.05$, and (c) $\omega_2 = 0.1$. Other parameters in the MFSPM are fixed at $\alpha = -0.5$, $\beta_1 = 0.6$, $\omega_1 = 0.01$, and $\beta_2 = 0.3$. In (b) and (c), the function $\beta_2\cos(\omega_2 t) - 1.5$ is superimposed, clearly showing that $\omega_e = \omega_2$.

of the active phase, and thus AMB is created [e.g., see Figs. 4(b)–4(d)]. In particular, a larger value of ω_2 may lead the MFSPM to show more ups and downs in the active area. As a result, a higher oscillation frequency can be observed in the envelope of the active phase. Note that the ups and downs that the MFSPM exhibits are decided by the excitation $\beta_2\cos(\omega_2 t)$. Therefore, the envelope of the active phase has the same oscillation frequency as that of $\beta_2\cos(\omega_2 t)$, i.e., $\omega_e = \omega_2$ [e.g., see Figs. 4(b)–4(d)], where ω_e is the oscillation frequency of the envelope. Obviously, the modulating modes which the MFSPM exhibits do not depend on specific systems; thus, the result $\omega_e = \omega_2$ is general and can be applied to other dynamical systems as well, e.g., see the Examples 2 and 3.

We would like to point out that, a Hopf bifurcation delay behavior, i.e., the delay loss of stability of the rest state, appears when the slow parameter a (either single-frequency or multiple-frequency) increases through the Hopf bifurcation point (e.g., see Fig. 6). Such delay behavior prolongs the quasistationary process of bursting and forms a hysteresis between the unstable rest state and the active state. The termination of the delay leads to a catastrophic transition from the unstable rest state to the active state, which begins the active phase of bursting. Then, the active phase, whether its envelope shows oscillations or not, evolves under the control of the slow parameter.

Remark 1. The active phase of bursting may be "compressed" because the quasistationary process of bursting is prolonged by Hopf bifurcation delay. In this example, a positive α (i.e., $\alpha = 1$) is selected. This increases the staying time of the slow parameter a in the active area and thus extends the active phase. That is to say Fig. 4 shows bursting patterns with an extended active phase.

Example 2. We analyze now the three-dimensional circuit system (3). According to [14], Fig. 2(c) shows a typical dynamical evolution behavior of the system. So, based on the stabilities and bifurcations in Fig. 2(c), here we include the MFSPM on the control parameter d to explore the generation of AMB. Obviously, the active area $(d_{\mathrm{sup}H}, d_{LPC}) = (-0.9114, 0.8037)$, starting from the supercritical Hopf bifurcation point supH and ending at the fold bifurcation points LPCs of limit cycles, can be divided into two parts, i.e., the monostable active area $(d_{\mathrm{sup}H}, d_{\mathrm{sub}H}) = (-0.9114, 0.4557)$ and the multistable active area $(d_{\mathrm{sub}H}, d_{LPC}) = (0.4557, 0.8037)$, by the subcritical Hopf bifurcation point subH.

In the multistable active area, there are three attractors, which provide three possible objects that the trajectory jumps to after the termination of the Hopf bifurcation delay. Surely, this will dilute the subject and trouble our analysis. So, the monostable active area is chosen as the real active area of bursting.

To this end, the parameters α, $\beta_{1,2}$, and $\omega_{1,2}$ in the MFSPM can be selected properly based on conditions (a) and (b). For example, we choose $\alpha = -0.5$, $\beta_1 = 0.6$, and $\beta_2 = 0.3$, which indicates that the MFSPM is not able to enter the multistable active area, but to visit the monostable active area and the rest area. Note that the active state is the only attractor in the monostable active area, so the bursting trajectory will jump to the active state after Hopf bifurcation delay. Moreover, we fix $\omega_1 = 0.01$ and let the frequency ω_2 be increased from 0.01. Then a transition from a single-frequency slow parametric modulation to the MFSPM occurs, which thus leads

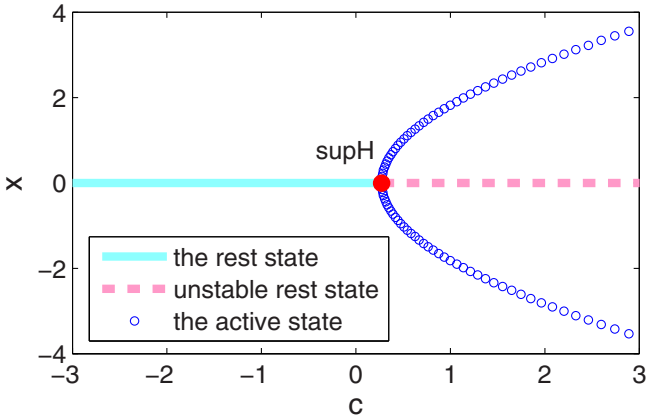

FIG. 8. A supercritical Hopf bifurcation supH with the bifurcation value $c_{\mathrm{sup}H} = 0.2727$ can be observed in system (5), where c is the control parameter.

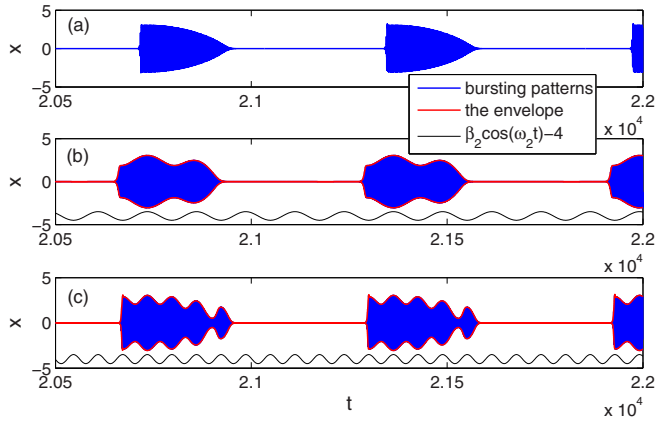

FIG. 9. The same as in Fig. 4 for system (5), where $a = 10$, $b = 2.67$, $k = 8$, $e = 1$, and c is the MFSPM, i.e., $c = \alpha + \beta_1\cos(\omega_1 t) + \beta_2\cos(\omega_2 t)$, where $\alpha = 0.8$, $\beta_1 = 1$, $\omega_1 = 0.01$, and $\beta_2 = 0.5$. In (a)–(c), the frequency ω_2 is fixed at $\omega_2 = 0.01,\ 0.05$, and 0.1, respectively. The function $\beta_2\cos(\omega_2 t) - 4$ further confirms the oscillation law of the envelope: $\omega_e = \omega_2$.

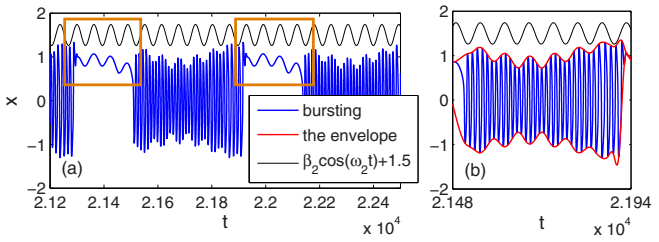

FIG. 10. AMB in system (3) (a) and its local enlargement (b). Here the rest state is the nonzero equilibrium E_+, the values of which rely on the system parameters [see Fig. Fig. 2(c)]. The MFSPM is $d = \alpha + \beta_1\cos(\omega_1 t) + \beta_2\cos(\omega_2 t)$, where $\alpha = 0.3$, $\beta_1 = 0.6$, $\omega_1 = 0.01$, $\beta_2 = 0.24$, and $\omega_2 = 0.1$. The parameters are the same as in Fig. 2(a). In (a) and (b), the function $\beta_2\cos(\omega_2 t) + 1.5$ is added, which shows that $\omega_q = \omega_2$ and $\omega_e = \omega_2$, respectively. Here ω_q denotes the oscillation frequency of the quasistationary process [see the rectangle areas in (a)].

the bursting to undergo a transition from a common type to the amplitude-modulated type (e.g., see Fig. 7). Similarly, a larger ω_2 means more oscillations, which show the same frequency as that of $\beta_2\cos(\omega_2 t)$ (i.e., $\omega_e = \omega_2$), in the envelope of the active phase [see Figs. 7(b) and 7(c)].

Example 3. Another example is the following four-dimensional hyperchaotic system [29],

$$\dot{x} = a(y - x), \quad \dot{y} = cx - y - xz + u,$$
$$\dot{z} = xy - bz, \quad \dot{u} = -kx + eyz, \tag{5}$$

where a, b, c, e, and k are the parameters. Zhou *et al.* [29] showed that this system exhibits a supercritical Hopf bifurcation under certain parameter conditions. For example, for the fixed parameters $a = 10$, $b = 2.67$, $k = 8$, and $e = 1$, a periodically active state can be observed in the certain parameter interval of c. When c is decreased from the parameter interval, the active state gradually shrinks and finally turns into a rest state, i.e., the stable origin, at the critical value $c_{\mathrm{sup}H} = 0.2727$, where a supercritical Hopf bifurcation takes place (see Fig. 8).

Based on the bifurcation behavior in Fig. 8, a common bursting pattern, resulting from Hopf bifurcation delay, is generated, and it will transit to patterns of amplitude-modulated type in the presence of the MFSPM (e.g., see Fig. 9). Besides, the envelope of the active phase follows the same oscillation law $\omega_e = \omega_2$ as discussed for Examples 1 and 2.

IV. CONCLUSION AND DISCUSSION

AMB is a novel class of bursting rhythms, and exploring possible routes to such bursting pattern is an important problem in the study of bursting systems. In this paper, we have proposed a basic approach for obtaining AMB by using the MFSPM. Generally, the active phase of bursting is related to the active state, whose amplitude often shows a simple variety law, which thus cannot lead to oscillations in the envelope of the active phase directly. However, it becomes quite different in the presence of the MFSPM. Our study shows that, under certain conditions, the MFSPM leads to to-and-fro varyings of the amplitude of the traced active state, gives rise to oscillations in the envelope of the active phase, and finally creates AMB. Based on this, the approach for obtaining AMB by the MFSPM is proposed. Besides, the excitation frequencies have been found to have strong effects on AMB: If one of the excitation frequencies is an integer multiple of the other one, the envelope has the same oscillation frequency as that of the excitation with relatively high frequency.

All of the AMB patterns obtained here show a basic property; i.e., the rest state related to the quasistationary process of bursting does not rely on the system parameters, but is fixed at some constant value. Therefore, the quasistationary process does not show oscillations (see Figs. 4, 7, and 9), though multiple ups and downs can also be observed in the rest area [e.g., see Figs. 5(b)–5(d)]. If the rest state depends on the system parameters, however, the case may become different. For this case, the bursting trajectory will follow such a rest state, the values of which alternate between increase and decrease, and this will lead to oscillations in the quasistationary process of bursting. Moreover, it is easy to see that, besides the active phase of bursting, the quasistationary process of bursting has the same oscillation frequency as that of the excitation with relatively higher frequency (see Fig. 10).

Another common property is that here all the AMB patterns are based on a Hopf bifurcation and its delay behavior. In fact, besides Hopf bifurcation, lots of bifurcations may lead to bursting. Note that the evolution modes that the MFSPM exhibits, however, do not depend on specific bifurcations. Therefore, oscillations can also be observed in the envelope of the active phase for the case when the bursting involves other bifurcations. Based on this, one may conclude that AMB is ubiquitous in dynamical systems modulated by the MFSPM.

Finally, we point out that our analytical treatment may be extended to applications, where a slow, multiple scale driving is relevant. An actual example may be a recent exciting discovery in biology [30], related to the evolution of vocal diversity of a group of bird species with the largest number of sound sources in all the animal kingdom. According to [30], the bronchial labia of the birds involved would be the dynamical system, and the forcing with two time scales would be the

air-sac pressure (very low modulation of the pressure below the syringeal membranes) and the upper pressure modulation by the tracheal membrane's oscillations. As previously described, these dynamical effects end up in the modulation of the bursting, interpreting each bout as a burst of syringeal oscillations, and therein lies the generation of amplitude-modulated acoustic features that are independent of complex neuromuscular control.

ACKNOWLEDGMENTS

The authors express their gratitude to the anonymous reviewers whose comments have helped improve this paper. This work is supported by the National Natural Science Foundation of China (Grants No. 11572141, No. 11632008, No. 11772161, and No. 11502091) and the Training Project for Young Backbone Teacher of Jiangsu University.

[1] I. Elizalde and J. Ancheyta, Fuel **138**, 45 (2014).
[2] J. C. Tzou, M. J. Ward, and T. Kolokolnikov, Physica D **290**, 24 (2015).
[3] R. Monopoli, IEEE Trans. Autom. Control **12**, 80 (2003).
[4] A. Franceschini, E. Filippidi, E. Guazzelli, and D. J. Pine, Phys. Rev. Lett. **107**, 250603 (2011).
[5] A. N. Pisarchik, Phys. Lett. A **242**, 152 (1998).
[6] B. E. MartÍlnez-Zérega, A. N. Pisarchikb, and L. S. Tsimringb, Phys. Lett. A **318**, 102 (2003).
[7] A. N. Pisarchik and B. K. Goswami, Phys. Rev. Lett. **84**, 1423 (2000).
[8] A. N. Pisarchik, B. F. Kuntsevich, and R. Corbalán, Phys. Rev. E **57**, 4046 (1998).
[9] A. N. Pisarchik, V. N. Chizhevsky, R. Corbalán, and R. Vilaseca, Phys. Rev. E **55**, 2455 (1997).
[10] L. Holden and T. Erneux, SIAM J. Appl. Math. **53**, 1045 (1993).
[11] G. J. M. Maree, SIAM J. Appl. Math. **56**, 889 (1996).
[12] D. C. Diminnie and R. Haberman, J. Nonlinear Sci. **10**, 197 (2000).
[13] X. J. Han, Q. S. Bi, C. Zhang, and Y. Yu, Int. J. Bifurcation Chaos Appl. Sci. Eng. **24**, 1450098 (2014).
[14] X. J. Han, F. B. Xia, P. Ji, Q. S. Bi, and J. Kurths, Commun. Nonlinear Sci. Numer. Simul. **36**, 517 (2016).
[15] J. Y. Hou, X. H. Li, D. W. Zuo, and Y. N. Li, Eur. Phys. J. Plus **132**, 283 (2017).
[16] E. M. Izhikevich, Int. J. Bifurcation Chaos Appl. Sci. Eng. **10**, 1171 (2000).
[17] B. Ibarz, J. M. Casado, and M. A. F. Sanjuán, Phys. Rep. **501**, 1 (2011).
[18] M. Desroches, J. Guckenheimer, B. Krauskopf, C. Kuehn, H. M. Osinga, and M. Wechselberger, SIAM Rev. **54**, 211 (2012).
[19] C. Kuehn, *Multiple Time Scale Dynamics* (Springer, Berlin, 2015).
[20] T. Vo, M. A. Kramer, and T. J. Kaper, Phys. Rev. Lett. **117**, 268101 (2016).
[21] T. Vo, Physica D **356-357**, 37 (2017).
[22] K. Tsaneva-Atanasova, H. M. Osinga, T. Rieß, and A. Sherman, J. Theor. Biol. **264**, 1133 (2010).
[23] J. Burke, M. Desroches, A. Granados, T. J. Kaper, M. Krupa, and T. Vo, J. Nonlinear Sci. **26**, 405 (2016).
[24] K. L. Roberts, J. E. Rubin, and M. Wechselberger, SIAM J. Appl. Dyn. Syst. **14**, 1808 (2015).
[25] Q. S. Lu, H. G. Gu, Z. Q. Yang, X. Shi, L. X. Duan, and Y. H. Zheng, Acta Mech. Sin. **24**, 593 (2008).
[26] A. E. Matouk and H. N. Agiza, J. Math. Anal. Appl. **341**, 259 (2008).
[27] D. C. Braga, L. F. Mello, and M. Messias, Math. Probl. Eng. **2009**, 149563 (2009).
[28] Y. A. Kuznetsov, *Elements of Applied Bifurcation Theory* (Springer, New York, 1995).
[29] L. L. Zhou, Z. Q. Chen, Z. L. Wang, and J. Z. Wang, Chaos, Solitons Fractals **91**, 148 (2016).
[30] S. M. Garcia, C. Kopuchian, G. B. Mindlin, M. J. Fuxjager, P. L. Tubaro, and F. Goller, Curr. Biol. **27**, 2677 (2017).